Comparison of Reaction Centers from *Rhodobacter sphaeroides* and *Rhodopseudomonas viridis*: Overall Architecture and Protein–Pigment Interactions†

Ossama El-Kabbani,‡,§ Chong-Hwan Chang,‖ David Tiede,‡ James Norris,‡ and Marianne Schiffer*,‖
Biological and Medical Research Division and Chemistry Division, Argonne National Laboratory, Argonne, Illinois 60439
Received October 30, 1990; Revised Manuscript Received February 6, 1991

ABSTRACT: Photosynthetic reaction centers (RCs) from the photosynthetic bacteria *Rhodobacter sphaeroides* and *Rhodopseudomonas viridis* are protein complexes closely related in both structure and function. The structure of the *Rps. viridis* RC was used to determine the structure of the RC from *Rb. sphaeroides*. Small but meaningful differences between the positions of the helices and the cofactors in the two complexes were identified. The distances between helices A_L and A_M, between B_L and B_M, and between bacteriopheophytins BP_L and BP_M are significantly shorter in *Rps. viridis* than they are in *Rb. sphaeroides* RCs. There are a number of differences in the amino acid residues that surround the cofactors; some of these residues form hydrogen bonds with the cofactors. Differences in chemical properties and location of these residues account in some manner for the different spectral properties of the two RCs. In several instances, the hydrogen bonds, as well as the apparent distances between the histidine ligands and the Mg atoms of the bacteriochlorophylls, were found to significantly differ from the *Rb. sphaeroides* RC structure previously described by Yeates et al. [(1988) *Proc. Natl. Acad. Sci. U.S.A. 85*, 7993–7997] and Allen et al. [(1988) *Proc. Natl. Acad. Sci. U.S.A. 85*, 8487–8491].

The molecular structures of the photosynthetic reaction centers (RC) from two purple bacteria, *Rhodopseudomonas viridis* and *Rhodobacter sphaeroides*, have been determined (Deisenhofer et al., 1985a; Chang et al., 1986; Allen et al., 1986; Deisenhofer & Michel, 1989; Feher et al., 1989). While they are very similar in their structures and spectral properties, a number of differences exist. Their similarities and differences contain clues about both membrane proteins in general and the mechanism of how light energy is converted into chemical energy by this molecule. Further, the spectral properties of the two RCs must be related to the nature of the cofactors and to the amino acid residues that surround the individual cofactors.

The *Rps. viridis* RC has four protein subunits: the L, M, and H chains and a four-heme cytochrome. It contains four bacteriochlorophyll *b* molecules, two bacteriopheophytin *b* molecules, a menaquinone, an ubiquinone, and a non-heme iron atom. The *Rb. sphaeroides* RC has only three protein subunits, the L, M, and H chains. It contains four bacteriochlorophyll *a* molecules, two bacteriopheophytin *a* molecules, two ubiquinones, and a non-heme iron atom. The L chain has 273 amino acids in *Rps. viridis* and 281 amino acids in *Rb. sphaeroides*. The eight additional residues in the *Rb. sphaeroides* L chain are located at its C-terminus; 59% of the amino acids of the L chains are identical in the two structures (Williams et al., 1984; Michel et al., 1986a). The M chain in *Rps. viridis* RC has 323 amino acids; it has 18 extra residues at its C-terminus compared with *Rb. sphaeroides*. The extra chain segment in *Rps. viridis* is used to anchor the cytochrome subunit. The M chain in *Rb. sphaeroides* has 307 residues, with two single amino acid insertions compared with the *Rps. viridis* M chain; one insertion is before the A helix and the other before the B helix. Fifty percent of the amino acids of the M chains of the two species are identical (Williams et al., 1983; Michel et al., 1986a). While the lengths of the H chains are similar (260 residues in *Rb. sphaeroides* and 258 residues in *Rps. viridis*), the overall sequence identity is only 39%; several insertions and deletions of chain segments are required for optimal alignment of the two sequences (Michel et al., 1985; Williams et al., 1986).

The L and M chains are transmembrane proteins with homologous structures and amino acid sequences. Each chain has five transmembrane helices, A, B, C, D, and E, and other short helical segments CD and DE (Deisenhofer et al., 1985a). The L and M chains are related to each other in the complex by a local 2-fold axis. Embedded in the L and M chains are nonprotein cofactors; two bacteriochlorophylls form the so-called "special pair" (BC_{LP} and BC_{MP}). Two monomeric "accessory" bacteriochlorophylls (BC_{LA} and BC_{MA}), two bacteriopheophytins (BP_L and BP_M), two quinones (Q_A and Q_B), and a non-heme iron atom comprise the remaining nonprotein components of the electron transfer system.

The differences in the absorption spectra of the bacteriochlorophylls and bacteriopheophytins in the two RCs are partially accounted for by the differences in the absorption maxima of the free pigments. The reason for the larger shift of the absorption of the special pair in *Rps. viridis* compared to *Rb. sphaeroides* is not clear at present. The rate of electron transfer is very similar in the two RCs at room temperature (Breton et al., 1988). The triplet state in the *Rb. sphaeroides* is symmetrically distributed on the two monomers of the special pair, while in *Rps. viridis*, the triplet state is located on the L-side monomer (Norris et al., 1989).

In the previous paper (Chang et al., 1991), we have discussed some overall properties of the *Rb. sphaeroides* structure; here, we emphasize the differences between the RCs from the

† C.-H.C. and M.S. were supported by the U.S. Department of Energy, Office of Health and Environmental Research, under Contract No. W-31-109-ENG-38 and by Public Health Service Grant GM36598; O.E.-K., D.T., and J.N. were supported by the U.S. Department of Energy, Division of Chemical Sciences, Office of Basic Energy Sciences, under Contract No. W-31-109-ENG-38.
‡ Chemistry Division.
§ Present address: Center for Macromolecular Crystallography, University of Alabama at Birmingham, University Station, Birmingham, AL 35294.
‖ Biological and Medical Research Division.

0006-2960/91/0430-5361$02.50/0

two organisms and also compare our structure to the *Rb. sphaeroides* structure determined by Yeates et al. (1988) and Allen et al. (1988).

Materials and Methods

Summary of Crystallization Conditions, Structure Determination, and Refinement of the Three RC Structures. Rps. viridis RC (Deisenhofer & Michel, 1989): crystals were grown from 2.2–2.4 M ammonium sulfate, in the presence of *N,N*-dimethyldodecylamine *N*-oxide (LDAO) and 3% heptane-1,2,3-triol. The unit cell is tetragonal $P4_32_12$ with dimensions $a = b = 223.5$ Å and $c = 113.6$ Å. Data were collected at the synchrotron source in Hamburg (DESY) at 0 °C. Five different heavy atom derivatives were used to calculate the protein phases to 3 Å. After solvent flattening, the model of the complex was built and was refined by using 2.3-Å data with the programs PROTEIN, EREF, and TNT (Deisenhofer et al., 1985b; Tronrud et al., 1987). The *R* factor is 19.3% for 95 762 reflections to 2.3-Å resolution. The mean coordinate error for 10 288 non-hydrogen atoms was estimated to be 0.26 Å from a Luzzati plot (Luzzati, 1952). The refined coordinates used in the comparisons were generously provided by Dr. J. Deisenhofer and Dr. H. Michel.

Rb. sphaeroides-R26 RC (Allen et al., 1986, 1987; Yeates et al., 1988): The protein was isolated with LDAO and crystallized with PEG 4000 in the presence of LDAO, ~0.5 M NaCl, 15 mM Tris (pH 8), and 3.9% heptanetriol. After the crystals were grown, the LDAO was exchanged for octyl β-glucoside. The unit cell is orthorhombic $P2_12_12_1$ with dimensions $a = 138.0$ Å, $b = 77.5$ Å, and $c = 141.8$ Å. Data were collected at the synchrotron source at Brookhaven. The structure was determined by molecular replacement using the partially refined coordinates of the *Rps. viridis* RC from 1985 (Deisenhofer et al., 1985a). Refinement was carried out with PROLSQ (Hendrickson, 1985). The *R* factor was 24% for 23 349 reflections to 2.8-Å resolution. The mean coordinate error was estimated to be 0.5 Å from Read's Q_A plot (Read, 1986). For the comparisons, published information about the structure was used.

Rb. sphaeroides-R26 RC (Chang et al., 1985, 1991): The protein was isolated with octyl β-glucoside and crystallized with PEG 4000 in the presence of octyl β-glucoside, 0.3 M NaCl, and 10 mM tris (pH 8). The unit cell is orthorhombic $P2_12_12_1$ with dimensions $a = 142.2$ Å, $b = 139.6$ Å, and $c = 78.7$ Å. Data were collected at the synchrotron source at Stanford (SSRL). The structure was determined by molecular replacement using the partially refined coordinates of the *Rps. viridis* RC from 1985 (Deisenhofer et al., 1985a). The refinement was carried out with programs PROLSQ (Hendrickson, 1985) and TNT (Tronrud et al., 1987). The *R* factor was 22% for 13 493 reflections to 3.1-Å resolution. The mean coordinate error was estimated to be 0.5 Å from a Luzzati plot (Luzzati, 1952). The refined coordinates were used in the comparisons.

Superposition Program. For the superposition of the *Rps. viridis* and *Rb. sphaeroides* coordinates, we used the least-squares program LSROTMOL, written by Dr. W. Steigemann. The program compares two similar molecules; it minimizes the square of the distances between equivalent atoms.

Labeling of the Amino Acid Residues. In order to simplify the comparisons, we have labeled the *Rb. sphaeroides* amino acid residues of the M chain according to the *Rps. viridis* sequence, following the alignment described by Michel et al. (1986a).

Center of Mass Calculations. Center of mass for the helices were calculated by using α-carbon atoms of the following residues: A helix (L33–L55, M53–M75), B helix (L84–L110, M111–M137), C helix (L116–L139, M143–M166), D helix (L171–L196, M198–M223), E helix (L226–L249, M260–M283), CD helix (L152–L162, M179–M189), and DE helix (L209–L220, M243–M254). The center of mass of the four nitrogen atoms of the pigments was taken as their center of mass.

Table I: Comparison of Positions of Helices and Pigments between *Rps. viridis* and *Rb. sphaeroides* Reaction Centers

	Δ[a]		distances (Å) between CMs of helices and pigments of L and M		
	L side	M side	*sph*[b]	*vir*[c]	difference
		Helices			
A	0.5	0.4	57.8	57.1	0.7
B	0.6	0.7	48.4	47.6	0.8
C	0.3	0.4	35.6	35.3	0.3
D	0.1	0.2	9.3	9.4	0.1
E	0.1	0.2	20.1	19.9	0.2
CD	0.6	0.3	16.8	16.8	0.0
DE	0.3	0.2	30.3	30.2	0.1
		Pigments			
special pair	0.6	0.5	6.7	6.6	0.1
acc chl[d]	0.5	1.4	22.2	22.0	0.2
pheophytin	0.8	0.8	23.9	23.1	0.8

[a] Δ = difference (in angstroms) in center of mass position between *Rb. sphaeroides* and *Rps. viridis* RCs after the superposition of the two molecules. [b] *Rb. sphaeroides*. [c] *Rps. viridis*. [d] Accessory bacteriochlorophyll.

Results and Discussion

Comparison of the Helical Architecture of the RC from Rps. viridis and Rb. sphaeroides

To compare the overall geometry of the RCs from *Rps. viridis* and *Rb. sphaeroides*, the two structures were superimposed by using the α-carbon atoms of the 10 transmembrane helices. (The *Rps. viridis* RC was placed into the *Rb. sphaeroides* unit cell.) Table I lists the differences after superposition between the locations of centers of mass for the helices and pigments in *Rps. viridis* and in *Rb. sphaeroides*, as well as the distances between the equivalent helices and pigments of the L and M subunits in the two species. The small observed differences in the geometries of RCs from the two species are meaningful because they are based on differences in the positions of the centers of mass of the pigments and helices. Further, though there were no symmetry restraints during refinement; as is discussed below, both the helices and the pigments moved in a symmetrical manner.

The relative positions of the D and E transmembrane helices in the two molecules are conserved; the D_L–D_M and E_L–E_M helix separations are the same. Further from the 2-fold axis, the location of the A and B helices differs by about 0.5 Å between *Rps. viridis* and *Rb. sphaeroides* on both the L and M side. The distance between the B helices is 0.8 Å larger and that of the A helices is 0.7 Å larger in *Rb. sphaeroides* than in *Rps. viridis* RC. The relative positions of the C helices, the central helix of each subunit, differ by about 0.3 Å, and the distance between the C helices is 0.3 Å larger in *Rb. sphaeroides* than in *Rps. viridis*. Though the distances between the CD helices and between the DE helices of the two subunits of the two species are the same, the individual helices moved relative to each other in *Rb. sphaeroides* and *Rps. viridis*.

From the above analysis, it appears that the maintenance of the geometry of the helices near the 2-fold axis, D and E of both subunits, is required for the function of the molecule. These are the core helices that form the main contacts with

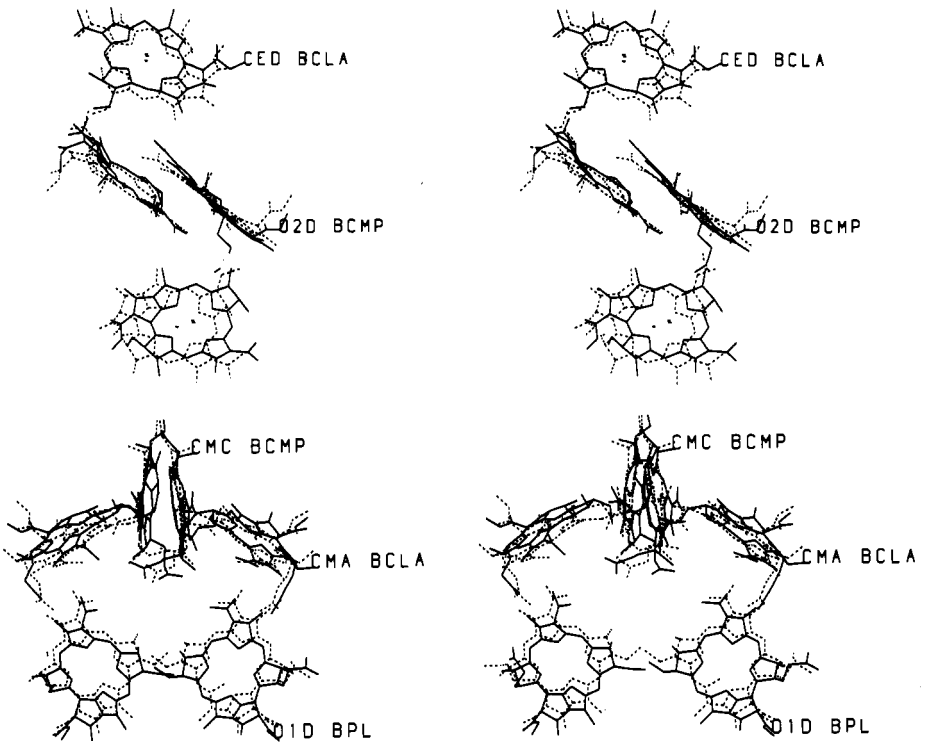

FIGURE 1: Comparison of the relative geometries of the bacteriochlorophylls and the bacteriopheophytins in *Rps. viridis* (broken lines) and *Rb. sphaeroides* (solid lines) reaction centers. (Top) Viewed along the local 2-fold axis; (bottom) viewed perpendicular to the local 2-fold axis.

the chromophores. On the other hand, there is more flexibility in the positions of the A and B helices, which are further away from the 2-fold axis and do not contact the chromophores. The movement relative to each other of the helices CD and DE in the two species might reflect the different mode of binding of some of the pigments.

The comparison of the bacteriochlorophyll and bacteriopheophytin positions of the two species (Table I) shows that they moved more relative to each other than did the helices. The largest shift of 1.4 Å is in the position of BC_{MA}. This can be explained by the fact that the *Rps. viridis* RC contains a carotenoid located close to BC_{MA} while the R-26 mutant of the *Rb. sphaeroides* used in this study does not have a carotenoid. In spite of the change in position of the bacteriochlorophylls in the two species, the distance between the pigments on the M and L sides is maintained. The planes of the BC_{LA} and BC_{MA} macrocycles in *Rps. viridis* are parallel to but located "under" the planes found in *Rb. sphaeroides*; i.e., in *Rps. viridis*, they are further away from the periplasmic side of the membrane and are closer to the phytins (Figure 1). In addition, BC_{MA} in *Rps. viridis* is displaced (compared to its position in *Rb. sphaeroides*) toward atom NA along a line that connects the atoms NA and NC in the bacteriochlorophyll rings II and IV. Both bacteriopheophytins in *Rps. viridis* changed positions by 0.8 Å relative to those found in *Rb. sphaeroides*. Also, the distance of the two bacteriopheophytins in *Rps. viridis* is 0.8 Å shorter than the equivalent distance in *Rb. sphaeroides*. The bacteriopheophytins in *Rps. viridis* are in approximately the same plane as they are in *Rb. sphaeroides*, but they are placed closer to the 2-fold axis and the special pair. Both bacteriopheophytins in *Rps. viridis* are displaced approximately along a line connecting atoms NB and ND of the macrocycles in the direction of NB atoms (line connecting ring I with ring III in the direction of ring I). This shift brings the ring I acetyl carbonyls of the bacteriopheophytins closer to the accessory chlorophylls in *Rps. viridis* on both sides of the complex.

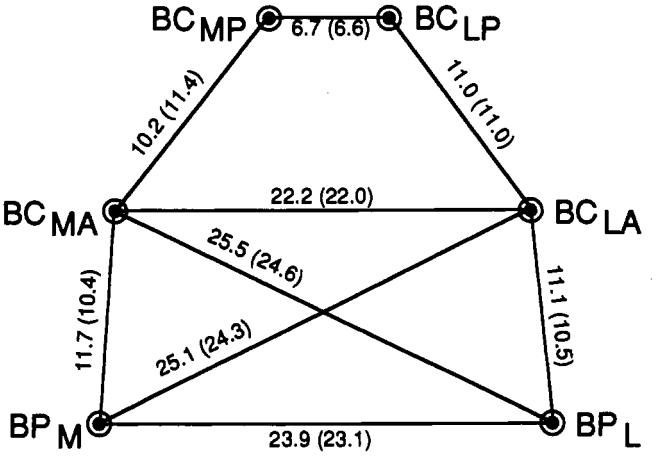

FIGURE 2: Distances between the pigments in the RCs from *Rb. sphaeroides* and *Rps. viridis* (shown in brackets).

In general as is shown in Figures 1 and 2, the bacteriopheophytins in *Rps. viridis* are closer to the accessory bacteriochlorophylls and to the special pair than they are in *Rb. sphaeroides*. The distribution of the pigments in *Rps. viridis* is more compact than it is in *Rb. sphaeroides*. The distance between BC_{LP} and BC_{LA} is the same in both species, while the distance in *Rb. sphaeroides* is longer between BC_{LA} and BP_L and between BC_{MA} and BP_M. The difference in the distance between BC_{MP} and BC_{MA}, where it is longer in *Rps. viridis*, probably reflects the presence or absence of the carotenoid moiety of the RC. The closer pigment distances in *Rps. viridis* correlate with faster electron transfer at cryogenic temperatures (Breton et al., 1988).

Protein–Cofactor Interactions: Comparison of the Interactions between Rps. viridis and Rb. sphaeroides RCs

Protein–Special Pair Interactions. The special pair is located close to the periplasmic side of the complex in a hy-

Table II: Amino Acid Residues That Surround the Special Pair[a]

	BC_{LP}					BC_{MP}			
	Rb. sphaeroides		*Rps. viridis*			*Rb. sphaeroides*		*Rps. viridis*	
position	residue	*d* (Å)	residue	*d* (Å)	position	residue	*d* (Å)	residue	*d* (Å)
L127	A	4.7	M	3.0	M154	L	3.0	**F**	3.5
L131	L	4.8	L	4.1	M158	L	2.7	I	4.2
L156	**W**	3.5	**W**	5.1	M183	**W**	4.6	**W**	4.0
L157	V	3.9	V	3.6	M184	Thr	3.1	L	3.6
L158	Ser	5.0	Asn	4.1	M185	Asn	4.3	Thr	3.9
L160	Thr	4.6	**F**	3.4	M187	**F**	3.1	**F**	4.0
L161	G	4.2	G	3.9	M188	Ser	3.2	Ser	3.7
L162	**Tyr**	3.1	**Tyr**	4.0	M189	L	7.0	I	6.2
L167	**F**	4.3	**W**	3.5	M194	L	3.1	**F**	3.3
L168	**His***	2.6	**His***	2.8	M195	**F**	3.0	**Tyr***	3.2
L173	**His**	3.1	**His**	2.2	M200	**His**	2.2	**His**	1.9
L176	A	4.2	Ser	3.2	M203	Ser	4.0	Ser	3.7
L177	I	3.1	V	3.7	M204	I	3.1	I	3.3
L180	**F**	3.1	L	3.8	M207	L	4.0	A	4.0
L181	**F**	4.3	**F**	3.8	M208	**Tyr**	3.5	**Tyr**	3.4
L240	A	5.9	I	4.0	M274	V	5.3	V	4.5
L244	Ser	2.6	G	3.3	M278	G	3.3	A	3.2
L247	Cys	5.1	G	4.0	M281	G	5.5	G	4.4
L248	M	3.1	Thr*	2.6	M282	I	3.4	I	3.7
M208	**Tyr**	3.2	**Tyr**	3.0	L181	**F**	3.0	**F**	3.3

[a] Nonpolar residues are listed by their one-letter codes, aromatic residues are listed in boldface type, and ionizable or polar residues are listed by their three-letter codes. The residues that are hydrogen bonded to the chromophores are marked by asterisks. The table lists the closest distance between the pigments and amino acid residues; the atoms involved are not necessarily the same ones in both RCs.

Table III: Amino Acid Residues That Surround the Accessory Chlorophylls[a]

	BC_{LA}					BC_{MA}			
	Rb. sphaeroides		*Rps. viridis*			*Rb. sphaeroides*		*Rps. viridis*	
position	residue	*d* (Å)	residue	*d* (Å)	position	residue	*d* (Å)	residue	*d* (Å)
L97	**F**	5.3	**F**	4.6	M124	V	8.0	L	6.4
L127	A	7.1	M	5.3	M154	L	4.7	**F**	3.8
L128	**Tyr**	3.1	**F**	3.7	M155	**W**	4.5	V	3.6
L131	L	3.3	L	4.4	M158	L	3.1	I	4.1
L146	**F**	3.2	**F**	3.7	M173	V	3.1	V	4.0
L148	**Tyr**	6.6	**Tyr**	5.8	M175	**Tyr**	5.9	**F**	5.5
L150	I	5.9	I	3.5	M177	I	5.3	I	3.7
L151	**W**	4.5	L	4.1	M178	**F**	6.7	**W**	3.4
L153	**His**	2.9	**His**	2.2	M180	**His**	2.6	**His**	2.1
L154	L	3.2	L	3.8	M181	L	3.6	I	3.0
L156	**W**	4.5	**W**	4.6	M183	**W**	3.1	**W**	4.3
L157	V	3.9	V	3.7	M184	Thr	3.5	L	3.8
M195	**F**	3.1	**Tyr**	3.7	L168	**His**	3.0	**His**	3.6
M201	G	4.3	G	3.4	L174	M	3.1	M	3.6
M204	I	4.0	I	3.4	L177	I	3.0	V	3.8
M205	A	3.2	G	3.4	L178	Ser*	3.1	Ser	3.4
M208	**Tyr**	4.6	**Tyr**	3.4	L181	**F**	5.2	**F**	3.7

[a] The same conventions are employed as in Table II.

drophobic environment formed by residues of the L and M subunits. The planes of their macrocycles are nearly parallel to each other and to the local 2-fold axis. The special pair is in contract with residues from the C, D, E, and CD helices of the L and M subunits. Table II lists the amino acid residues that surround the special pair in *Rb. sphaeroides* and *Rps. viridis* and the minimum distance between each monomer and the side chains of the corresponding residues. The amino acid residues in contact with the special pair in *Rb. sphaeroides* include fewer aromatic side chains and residues that can hydrogen bond than those in *Rps. viridis*.

The special locations and different chemical characters of Tyr M208 and the symmetry-related residue Phe L181 were noted by Tiede et al. (1988). Tyr M208 is found between the special pair, the monomeric bacteriochlorophyll, and the bacteriopheophytin of the L side. The aromatic ring of Tyr M208 is within van der Waals distance of the corresponding macrocycles. The corresponding Phe L181 forms similar interactions with the special pair, the monomeric bacteriochlorophyll, and bacteriopheophytin of the M side (see Tables III and IV). An additional hydrogen bond in *Rb. sphaeroides* between Tyr M208 and the propionic acid carbonyl of ring IV of BC_{LP} has been reported by Yeates et al. (1988). No such hydrogen bond is observed in our refined *Rb. sphaeroides* model; the shortest distance between the OH of the tyrosine side chain and the BC_{LP} propionic acid carbonyl of ring IV is 5.4 Å.

The central Mg atoms of BC_{LP} and BC_{MP} are liganded to the NE2 atoms of histidines L173 and M200 of the D helices. In *Rps. viridis*, the distances between the two Mg^{2+} atoms and their histidine ligands are 2.2 and 1.9 Å, respectively. In *Rb. sphaeroides*, we find corresponding distances of 3.2 and 2.2 Å. This compares with 4 Å and less than 3 Å reported by Yeates et al. (1988). In *Rps. viridis*, the ring I acetyl carbonyl oxygens of BC_{LP} and BC_{MP} are hydrogen bonded to His L168 and Tyr M195, respectively. The *Rb. sphaeroides* structure shows that a similar hydrogen bond (2.6 Å) is formed between the conserved His L168 (NE2) and the ring I acetyl of BC_{LP}

Table IV: Amino Acid Residues That Surround the Pheophytins[a]

	BP_L					BP_M			
	Rb. sphaeroides		*Rps. viridis*			*Rb. sphaeroides*		*Rps. viridis*	
position	residue	*d* (Å)	residue	*d* (Å)	position	residue	*d* (Å)	residue	*d* (Å)
L97	F	3.2	F	3.3	M124	V	3.9	L	3.5
L100	W*	3.1	W*	3.3	M127	W*	3.3	W*	3.2
L101	A	6.6	M	7.8	M128	W	6.9	W	7.2
L104	Glu*	2.8	Glu*	2.7	M131	Thr*	2.9	V	3.9
L117	I	4.2	V	3.8	M144	Thr	4.7	I	3.6
L118	P	5.6	P	5.7	M145	A	7.0	A	6.8
L121	F	3.4	F	3.4	M148	F	3.1	F	3.4
L124	A	3.9	P	3.4	M151	A	4.1	A	4.1
L237	Ser	4.7	A	4.4	M271	A	3.8	Ser	3.8
L238	L	4.7	Ser	5.0	M272	V	4.8	L	7.0
L240	A	6.3	I	4.8	M274	V	4.9	V	4.1
L241	V	4.1	F	3.5	M275	Thr	4.3	M	3.3
M208	Tyr	3.3	Tyr	3.0	L181	F	3.8	F	3.1
M209	G	7.3	G	6.7	L182	Thr	6.7	V	7.2
M212	L	4.0	L	3.5	L185	L	3.1	M	3.6
M215	A	3.9	A	4.1	L188	A	4.2	G	5.3
M216	M	4.3	A	4.1	L189	L	3.3	L	3.4
M250	W	3.1	W	3.6	L216	F	3.7	F	4.7
M253	Thr	4.3	Thr	4.3	L219	L	4.7	V	4.2
M254	M	3.3	I	3.8	L220	V	4.8	V	3.5

[a] The same conventions are employed as in Table II.

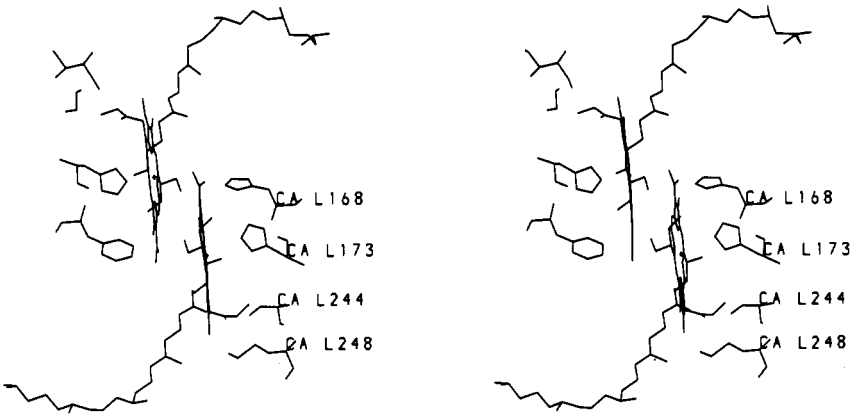

FIGURE 3: Stereo picture illustrates the location of residues near the special pair. His L173, His L168, Ser L244, and Met L248 are labeled. The symmetrical residues, His M200, Phe M195, Gly M278, and Ile M282 are not labeled. In the *Rps. viridis* RC, residue L244 is Ala, L248 is Thr, and M195 is Tyr.

(see Figure 3). In contrast, the residue at the symmetry-related position on the M side, Phe M195, cannot form a hydrogen bond to BC_{MP}. Thus, the symmetry in hydrogen bonding to the ring I acetyl groups in the bacteriochlorophyll dimer of *Rps. viridis* is not preserved in *Rb. sphaeroides*. It should be noted that, in X-ray diffraction studies, the orientation of an acetyl group is necessarily assigned on the basis of apparent hydrogen-bonding relationships since oxygen atoms and methyl groups are not distinguishable in electron density maps. Despite the absence of hydrogen bonding to the BC_{MP} ring I acetyl in *Rb. sphaeroides*, we assumed that the most likely configurations of both acetyl groups with respect to the macrocycle are equivalent. In the *Rb. sphaeroides* structure described by Yeates et al. (1988), His L168 forms a hydrogen bond with His L173 but not with the acetyl group of BC_{LP}; neither acetyl group of the bacteriochlorophylls is hydrogen bonded to the protein scaffolding.

In *Rb. sphaeroides*, Ser L244 is hydrogen bonded (2.8 Å) to the ester carbonyl of ring V of BC_{LP}. In *Rps. viridis*, L244 is a Gly that cannot hydrogen bond. The residues on the M side (Gly or Ala) also cannot form hydrogen bonds. An additional hydrogen bond is present in *Rps. viridis* between the keto carbonyl of ring V of BC_{LP} and Thr L248. In *Rb. sphaeroides*, Thr L248 is replaced by a Met which cannot form a hydrogen bond. The equivalent residue on the M-side is a conserved non-hydrogen-bonding Ile M282, making both monomers of the *Rb. sphaeroides* special pair equivalently non-hydrogen-bonded at the ring V keto position.

EPR studies on reaction center single crystals show that whereas the triplet state is essentially localized on BC_{LP} in *Rps. viridis*, it is distributed between both bacteriochlorophylls of the special pair in *Rb. sphaeroides* (Norris et al., 1989). Hydrogen-bonding patterns for the bacteriochlorophyll dimer in *Rps. viridis* and *Rb. sphaeroides* may be compared to measurements of localization of the excited triplet state (Norris et al., 1989). This comparison suggests that variation in hydrogen bonding of amino acids to the ring V keto position may be more important in perturbing the electronic structure of excited states than are changes in hydrogen bonding to the ring I acetyl groups. Further, the relative geometry of the two bacteriochlorophylls could be a more important factor than hydrogen bonding in determining the location of the triplet state.

Protein–Bacteriochlorophyll Monomer Interactions. The bacteriochlorophyll monomers BC_{LA} and BC_{MA} interact with the special pair and neighboring bacteriopheophytins. Amino acid residues from the B, C, D, and CD helices of the L and M subunits surround the monomers (see Table III). The two

histidines, L153 and M180, of the CD periplasmic helix are liganded to the central Mg^{2+} atoms of BC_{LA} and BC_{MA}, respectively. In *Rps. viridis*, the distances between the two Mg^{2+} atoms and the NE2 atoms of their histidine ligands are 2.2 and 2.1 Å. In *Rb. sphaeroides*, we observe the corresponding distances of 3.0 and 2.2 Å. The ND1 of the side chain of His L153 is also hydrogen bonded (2.6 Å) to the peptide carbonyl of Gly L149. Yeates et al. (1988) found that although His M180 coordinates to the Mg of BC_{MA}, His L153 on the L side does not; it forms only a hydrogen bond with the peptide carbonyl of L149.

No hydrogen bonds are observed between the bacteriochlorophyll monomers and the surrounding protein environment in *Rps. viridis*. The only hydrogen bond (3.1 Å) between the protein and the monomers in *Rb. sphaeroides* occurs between the hydroxyl of Ser L178 and the propionic acid carbonyl of ring IV of BC_{MA}; this was also reported by Yeates et al. (1988). The equivalent residue on the M side is an Ala, which cannot form a hydrogen bond. In *Rps. viridis*, though Ser L178 is conserved, its hydroxyl is too far away to form a similar hydrogen bond to the propionic acid carbonyl of ring IV of BC_{MA} (3.7 Å). Instead, it is hydrogen bonded to the peptide carbonyl of Met L174 (2.6 Å). In *Rb. sphaeroides*, the equivalent distance is 3.9 Å.

Rps. viridis and *Rb. sphaeroides* exhibit two differences in the conserved symmetry-related residues that are in van der Waals contacts with the accessory bacteriochlorophyll monomers (BC_{LA} and BC_{MA}). His L168, present in both species, forms a hydrogen bond with BC_{LP} and is in van der Waals contact with BC_{MA}. The equivalent residue in the *Rps. viridis* M chain, Tyr M195, makes similar interactions with BC_{MP} and BC_{LA} (see Tables II and III). However, Phe in *Rb. sphaeroides* cannot form a hydrogen bond. The conserved Phe L146 and the symmetry-related Val M173 are in van der Waals contacts with BC_{LA} and BC_{MA}, respectively.

Protein–Bacteriopheophytin Interactions. Each macrocycle of the two bacteriopheophytins (BP_L and BP_M) is located approximately at the center of the C and E helices and are oriented parallel to the D helix of its corresponding L or M subunit. BP_L and BP_M are in contact with residues from the D, E, B, and C membrane-spanning helices of the L and M subunits (see Table IV). The only ionizable residue near the macrocycles of the chromophores is the conserved residue, Glu L104. The side chain of Glu L104 is assumed to be protonated (Michel et al., 1986b) and forms a hydrogen bond (3 Å) with the keto carbonyl of ring V of BP_L. The symmetry-related residue Thr M131 also forms a similar hydrogen bond (2.9 Å) with the ring V keto carbonyl of the bacteriopheophytin on the M side; this hydrogen bond was also observed by Yeates et al. (1988). The equivalent residue in *Rps. viridis* is a valine, which cannot form a hydrogen bond. It was proposed earlier that the difference in hydrogen bonding at the ring V carbonyl position for *Rps. viridis* may contribute to the preferential use of the L pathway in electron transfer (Michel et al., 1986b). However, the fact that both bacteriopheophytins are hydrogen bonded at the ring V keto position in *Rb. sphaeroides* shows that hydrogen bonding alone cannot be the sole factor in determining the direction of electron transfer. A similar conclusion has also been drawn from mutagenesis experiments, where Glu L104 in *Rb. capsulatus* RCs has been replaced by glutamine and lysine residues (Bylina et al., 1988). In both of these mutants, the rates of electron transfer along the L pathway were only slightly modified (less than a factor of 2), and the yield of light-induced electron transfer along the L pathway was unaltered. These conclusions were also corroborated by electron transfer calculations based upon the *Rps. viridis* structure. Studies by Michel-Beyerle et al. (1988) suggested that the preferential use of the L pathway is predominately determined by relative positioning of the pigments and is only slightly enhanced by the presence of Glu L104. In *Chloroflexus aurantiacus*, Glu L104 is replaced by a noncharged Gln residue (Ovchinnikov et al., 1988).

The aromatic ring of Phe L97 makes van der Waals contact with the phytyl tails of both BP_L and BC_{LP}; symmetry-related aliphatic residues, M124 Leu in *Rps. viridis* and Val in *Rb. sphaeroides*, make a similar interaction with the pheophytin of the M side (see Table IV). As discussed above and by Tiede et al. (1988), the conserved Tyr M208 and symmetry-related Phe L181 are in van der Waals contact with the L- and M-chain monomers of the special pair and the bacteriopheophytins. The conserved Trp M250 and symmetry-related conserved Phe L216 are close to the pheophytins of the L and M sides. The indole ring of Trp M250 is in van der Waals distance of the BP_L macrocycle in both species, while Phe L216 is not.

The conserved residue Trp M127 is hydrogen bonded (3.0 Å) to the ester carbonyl of ring V of the M-side bacteriopheophytin. The symmetry-related Trp L100 is also conserved and has a similar interaction (3.1 Å) on the L side. Thus, we find the symmetry of hydrogen bonding appears to be maintained between the protein and the ring V ester group of the bacteriopheophytins in both species. Of potential photochemical significance, Yeates et al. (1988) found no hydrogen bond between Trp L100 and BP_L.

Protein–Quinone Interactions. The quinone Q_A is located near the BP_L and close to the cytoplasmic side of the RC. Q_A interacts with residues of the M subunit from the D and E membrane-spanning helices as well as with the DE helix (see Table V). In *Rps. viridis*, the two oxygens of the Q_A ring (menaquinone) are hydrogen bonded to the peptide nitrogen of Ala M258 and the side chain of His M217, respectively. Ala M258 forms a similar hydrogen bond (2.5 Å) with the O5 oxygens of the Q_A ring (ubiquinone) in *Rb. sphaeroides*, but the second oxygen (O2) is hydrogen bonded (2.4 Å) to the side chain of Thr M220 (see Figure 4). An additional hydrogen bond between the side chain of Thr M220 and the indole ring of Trp M250 in *Rb. sphaeroides* was reported by Allen et al. (1988). No hydrogen bond is present in our refined *Rb. sphaeroides* model, and the distance between NE1 of the Trp side chain and OH of the Thr side chain is 5.0 Å.

Near the Q_B site, residues from the M and H chains are present in addition to residues from the D, DE, and E helices of the L subunit. In *Rps. viridis*, there are hydrogen bonds between the two carbonyl oxygens of the Q_B ring and the side chains of His L190 and Ser L223. Similar hydrogen bonds to the two oxygens of the Q_B ring (ubiquinone) are observed in the *Rb. sphaeroides* structure (see Figure 4). The distance from ND1 of His L190 to O2 of Q_B is 2.9 Å, and that from OH of Ser L223 to O5 is 3 Å. The residue equivalent to Ser L223 on the M side is an Asn (M257), but it is too far to form a hydrogen bond with Q_A.

The residues that constitute the Q_B site make it far more polar than the Q_A site (see Table V). The acidic residue Glu L212 (and Asp L213 in *Rb. sphaeroides*) is part of the Q_B site. Glu L212 is assumed to be protonated and involved in the protonation of the reduced quinone after the photochemical reaction takes place (Michel et al., 1986a; Allen et al., 1988). In *Rb. sphaeroides*, the methoxy oxygen O3 of the Q_B ring is within a hydrogen-bonding distance (2.9 Å) of the side chain of Glu L212. The lower polarity of the Q_A pocket may con-

Table V: Amino Acid Residues That Surround the Quinones[a]

	Q_B					Q_A			
	Rb. sphaeroides		*Rps. viridis*			*Rb. sphaeroides*		*Rps. viridis*	
position	residue	d (Å)	residue	d (Å)	position	residue	d (Å)	residue	d (Å)
L186	A	4.8	A	7.0	M213	L	5.9	L	4.6
L189	L	5.0	L	3.8	M216	M	4.9	A	3.8
L190	**His***	2.9	**His***	2.7	M217	**His**	4.3	**His***	3.1
L193	L	3.6	L	3.6	M220	Thr*	2.4	Thr	3.3
L194	V	3.9	I	3.9	M221	I	3.6	I	4.8
L212	Glu*	2.8	Glu	2.9	M246	A	4.0	A	4.0
L213	Asp	5.3	Asn	3.4	M247	A	4.4	A	4.1
L215	**F**	4.1	**Tyr**	7.0	M249	**F**	7.3	**F**	6.7
L216	**F**	3.0	**F**	3.0	M250	**W**	2.6	**W**	3.3
L220	V	4.2	V	4.3	M254	M	2.7	I	4.2
L222	**Tyr**	5.4	**Tyr**	4.7	M256	**F**	4.4	**F**	3.9
L223	Ser*	3.0	Ser*	2.7	M257	Asn	4.1	Asn	4.1
L224	I	3.5	I	3.7	M258	A*	2.5	A*	3.5
L226	Thr	4.5	A	3.9	M260	M*	3.0	I	3.7
L229	I	3.2	I	3.7	M263	I	3.4	V	3.9
L230	**His**	6.5	**His**	4.8	M264	**His**	4.8	**His**	6.7
L232	L	4.6	L	4.7	M266	**W**	3.6	**W**	3.8

[a] The same conventions are employed as in Table II.

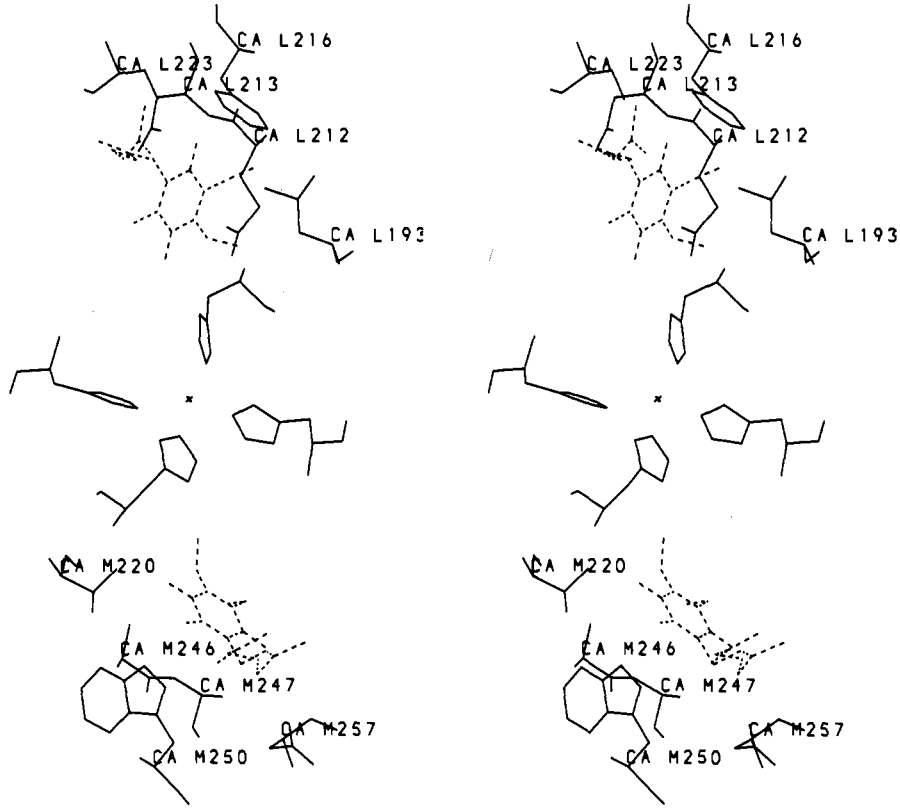

FIGURE 4: Residues around the quinones are illustrated. Residues that have different chemical characters in the two sites are labeled. Around the Q_A site, these are Thr M220, Ala M246, Ala M247, Trp M250, and Asn M257; the symmetry-related residues around the Q_B site are Leu L193, Glu L212, Asp L213, Phe L216, and Ser L223. Quinones are shown in broken lines.

tribute to the stronger binding of Q_A and the modification of its redox properties compared with Q_B.

A difference in the orientation of the side chains of Phe L216 and Trp M250 with respect to the secondary and primary quinone (Q_B and Q_A) rings is observed between the two species. In *Rps. viridis*, the aromatic rings of Phe L216 and Trp M250 are parallel to the Q_B and Q_A rings, respectively. On the other hand, in *Rb. sphaeroides*, Phe L216 is close to perpendicular to the quinone ring; it makes van der Waals contact with Q_B. Trp M250 makes an angle of 30° with Q_A and is almost parallel with Phe M149; this is different from that reported by Allen et al. (1988). Phe M256 and its symmetry-related Tyr L222 are in the vicinity of Q_A and Q_B, respectively (see Table V). The side chain of Tyr L222 is too far away to form a hydrogen bond with Q_B; it forms a hydrogen bond (3.0 Å) with the carbonyl oxygen of M43. The aromatic ring of Phe M256 and the indole ring of Trp M266 are near the tail of Q_A, while the equivalent smaller aliphatic residue on the L chain, Leu L232, is close to the tail of Q_B.

Interactions of Protein with Non-Heme Iron. The non-heme iron (Fe) lies approximately on the 2-fold symmetry axis relating the cofactors of the L and M sides. The iron is present between the Q_A and Q_B rings (see Figure 4) and is closer to the center of the Q_B ring by 0.8 and 0.7 Å in *Rps. viridis* and *Rb. sphaeroides*, respectively. Allen et al. (1988) found that Q_B is 2 Å closer to the iron than Q_A. Fe is liganded to the NE2 atoms of the side chains of four histidine residues from the D and E helices (L190, L230, M217, and M264) and one

Table VI: Significant Differences in *Rb. sphaeroides* Reaction Center Structures Reported Here and by Yeates et al. (1988) and Allen et al. (1988)

M208 Tyr H-bond with propionic carbonyl of ring IV of BC_{LP} (Yeates et al.)
not seen by us or in *Rps. viridis*

			this work	Yeates et al.	*Rps. viridis*
L173	His	-Mg distance	3.2	4.0	2.2
M200	His	-Mg distance	2.2	<3	1.9

L168 His H-bond with ring I acetyl of BC_{LP}, this work and in *Rps. viridis*
H-bonds with His L173 (Yeates et al.)

			this work	Yeates et al.	*Rps. viridis*
L153	His	-Mg distance	3.0	coordinates	2.2
M180	His	-Mg distance	2.2	does not coordinate	2.1

L100 Trp H-bonded to ester carbonyl of ring V of BP_L in this work and in *Rps. viridis* but not found by Yeates et al.

Difference in Fe–Q_B and Fe–Q_A Distance
Q_B is 0.8 Å closer in *Rps. viridis* to Fe than Q_A is
0.7 Å closer in this work
2.0 Å closer in Allen et al.

glutamic acid from the DE helix (M232). Glu M232 acts as a bidentate ligand for the Fe in *Rps. viridis*. In *Rb. sphaeroides*, at the present stage of refinement, the second oxygen of the side-chain carboxylate of Glu M232 appears to be too far away (3.3 Å) to be liganded to the Fe. These polar interactions between the Fe and the ligands of the L and M subunits may play an important role in stabilizing the tertiary structure of the RC complex. The imidazole rings of histidines L190 and M217 are located between the Fe and the Q_B ring and between the Fe and the Q_A ring, respectively. Although His L190 is hydrogen bonded to the Q_B ring in both species, His M217 is hydrogen bonded to the Q_A ring only in *Rps. viridis*.

Summary

Table VI summarizes significant differences between the RC structure determined by us and that published by Yeates et al. (1988) and Allen et al. (1988). The reason for the differences between the two structures is not clear. While they most likely include uncertainties in both structures, real differences between the two structures caused, for example, by subtle differences in crystallization conditions cannot be eliminated. Both of the *Rb. sphaeroides* RC structures were determined at medium resolution, and the estimated error in the atomic position is 0.5 Å, corresponding to a 0.7-Å error in the distance between two atoms (Yeates et al., 1988; Chang et al., 1991). Difference Fourier techniques do not work very well with medium-resolution data; feedback errors can lead to slightly different end results, depending on the exact course of the refinement. To understand the differences of the two *Rb. sphaeroides* RC structures, a detailed comparison of the diffraction data, as well as the atomic coordinates, will have to be carried out. Pooling of existing data sets and additional new data will ultimately be required to resolve apparent discrepancies. Further refinement of both structures by other methods such as molecular dynamics (X-PLOR) might also modify the details of the models.

Differences observed between the RC structures from *Rps. viridis* and *Rb. sphaeroides* are not surprising, because there are differences in their amino acid sequences and pigment compositions, though specific cause and effect cannot yet be identified. We are starting to probe the effect of differences in residues between *Rps. viridis* and *Rb. sphaeroides* RCs around the special pair by studying site-specific mutants of the *Rb. sphaeroides* RC in collaboration with J. Farchaus, J. Wachtveitl, and D. Oesterhelt, of the Max Planck Institute of Biochemistry.

Acknowledgments

We thank Dr. J. Deisenhofer and Dr. H. Michel for the refined *Rps. viridis* RC coordinates. We also thank Dr. F. J. Stevens and Dr. D. K. Hanson for many useful suggestions and for reviewing the manuscript.

References

Allen, J. P., Feher, G., Yeates, T. O., Rees, D. C., Deisenhofer, J., Michel, H., & Huber, R. (1986) *Proc. Natl. Acad. Sci. U.S.A. 83*, 8589–8593.
Allen, J. P., Feher, G., Yeates, T. O., Komiya, H., & Rees, D. C. (1987) *Proc. Natl. Acad. Sci. U.S.A. 84*, 5730–5734.
Allen, J. P., Feher, G., Yeates, T. O., Komiya, H., & Rees, D. C. (1988) *Proc. Natl. Acad. Sci. U.S.A. 85*, 8487–8491.
Breton, J., Martin, J.-L., Fleming, G. R., & Lambry, J.-C. (1988) *Biochemistry 27*, 8276–8284.
Bylina, E. J., Kirmaier, C., McDowell, L., Holten, D., & Youvan, D. C. (1988) *Nature 336*, 182–184.
Chang, C.-H., Schiffer, M., Tiede, D., Smith, U., & Norris, J. (1985) *J. Mol. Biol. 186*, 201–203.
Chang, C.-H., Tiede, D., Tang, J., Smith, U., Norris, J., & Schiffer, M. (1986) *FEBS Lett. 205*, 82–86.
Chang, C.-H., El-Kabbani, O., Tiede, D., Norris, J., & Schiffer, M. (1991) *Biochemistry* (preceding paper in this issue).
Deisenhofer, J., & Michel H. (1989) *EMBO J. 8*, 2149–2169.
Deisenhofer, J., Epp, O., Miki, R., Huber, R., & Michel, H. (1985a) *Nature 318*, 618–624.
Deisenhofer, J., Remington, S. J., & Steigemann, W. (1985b) *Methods Enzymol. 115*, 303–323.
Feher, G., Allen, J. P., Okamura, M. Y., & Rees, D. C. (1989) *Nature 339*, 111–116.
Hendrickson, W. (1985) *Methods Enzymol. 115*, 252–270.
Jack, A., & Levitt, M. (1978) *Acta Crystallogr., Sect. A 34*, 931–935.
Luzzati, P. V. (1952) *Acta Crystallogr. 5*, 802–810.
Michel, H., Weyer, K. A., Gruenberg, H., & Lottspeich, F. (1985) *EMBO J. 4*, 1667–1672.
Michel, H., Weyer, K. A., Gruenberg, H., Dunger, I., Oesterhelt, D., & Lottspeich, F. (1986a) *EMBO J. 5*, 1149–1158.
Michel, H., Epp, O., & Deisenhofer, J. (1986b) *EMBO J. 5*, 2445–2451.
Michel-Beyerle, M. E., Plato, M., Deisenhofer, J., Michel, H., Bixon, M., & Jortner, J. (1988) *Biochim. Biophys. Acta 932*, 52–70.
Norris, J. R., Budil, D. E., Gast, P., Chang, C.-H., El-Kabbani, O., & Schiffer, M. (1989) *Proc. Natl. Acad. Sci. U.S.A. 86*, 4335–4339.
Ovchinnikov, Yu A., Abdulaev, N. G., Zolotarev, A. S., Shmuckler, B. E., Zargarov, A. A., Kutuzov, M. A., Telezhinskaya, I. N., & Levina, N. B. (1988) *FEBS Lett. 231*, 237–242.
Read, R. J. (1986) *Acta Crystallogr., Sect. A 42*, 140–149.
Tiede, D. M., Budil, D. E., Tang, J., El-Kabbani, O., Norris, J. R., Chang, C.-H., & Schiffer, M. (1988) in *The Photosynthetic Bacterial Reaction Center* (Breton, J., & Vermeglio, A., Eds.) pp 13–20, Plenum, New York.
Tronrud, D. E., Ten Eyck, L. F., & Matthews, B. W. (1987) *Acta Crystallogr., Sect. A 43*, 489–501.

Williams, J. C., Steiner, L. A., Ogden, R. C., Simon, M. I., & Feher, G. (1983) *Proc. Natl. Acad. Sci. U.S.A. 80*, 6505–6509.
Williams, J. C., Steiner, L. A., Feher, G., & Simon, M. I. (1984) *Proc. Natl. Acad. Sci. U.S.A. 81*, 7303–7307.
Williams, J. C., Steiner, L. A., & Feher, G. (1986) *Proteins: Struct., Funct., Genet. 1*, 312–325.
Yeates, T. O., Komiya, H., Chirino, A., Rees, D. C., Allen, J. P., & Feher, G. (1988) *Proc. Natl. Acad. Sci. U.S.A. 85*, 7993–7997.

Identification of the Subunits of F_1F_O-ATPase from Bovine Heart Mitochondria‡

John E. Walker,* Renê Lutter,§,∥ Alain Dupuis,⊥ and Michael J. Runswick
Medical Research Council, Laboratory of Molecular Biology, Hills Road, Cambridge, CB2 2QH, U.K.
Received February 20, 1991

ABSTRACT: An oligomycin-sensitive F_1F_O-ATPase isolated from bovine heart mitochondria has been reconstituted into phospholipid vesicles and pumps protons. This preparation of F_1F_O-ATPase contains 14 different polypeptides that are resolved by polyacrylamide gel electrophoresis under denaturing conditions, and so it is more complex than bacterial and chloroplast enzymes, which have eight or nine different subunits. The 14 bovine subunits have been characterized by protein sequence analysis. They have been fractionated on polyacrylamide gels and transferred to poly(vinylidene difluoride) membranes, and N-terminal sequences have been determined in nine of them. By comparison with known sequences, eight of these have been identified as subunits β, γ, δ, and ϵ, which together with the α subunit form the F_1 domain, as the b and c (or DCCD-reactive) subunits, both components of the membrane sector of the enzyme, and as the oligomycin sensitivity conferral protein (OSCP) and factor 6 (F_6), both of which are required for attachment of F_1 to the membrane sector. The sequence of the ninth, named subunit e, has been determined and is not related to any reported protein sequence. The N-terminal sequence of a tenth subunit, the membrane component A6L, could be determined after a mild acid treatment to remove an α-*N*-formyl group. Similar experiments with another membrane component, the a or ATPase-6 subunit, caused the protein to degrade, but the protein has been isolated from the enzyme complex and its position on gels has been unambiguously assigned. No N-terminal sequence could be derived from three other proteins. The largest of these is the α subunit, which previously has been shown to have pyrrolidonecarboxylic acid at the N terminus of the majority of its chains. The other two have been isolated from the enzyme complex; one of them is the membrane-associated protein, subunit d, which has an α-*N*-acetyl group, and the second, surprisingly, is the ATPase inhibitor protein. When it is isolated directly from mitochondrial membranes, the inhibitor protein has a frayed N terminus, with chains starting at residues 1, 2, and 3, but when it is isolated from the purified enzyme complex, its chains are not frayed and the N terminus is modified. Previously, the sequences at the N terminals of the α, β, and δ subunits isolated from F_1-ATPase had been shown to be frayed also, but in the F_1F_O complex they each have unique N-terminal sequences. It is now apparent that the fraying of the α, β, and δ subunits arises when the F_1 particle is released from mitochondrial membranes and that the extent of fraying depends upon the method of release; proteolysis is less extensive when sonication rather than shaking with chloroform is employed. The sequences of the subunits of F_1F_O-ATPase show that eight of them are related to the subunits of the bacterial and chloroplast complexes, and presumably they have functions similar to those of their homologues. The ATPase inhibitor, F_6, and subunits ϵ, d, e and A6L have no obvious counterparts in bacteria and chloroplasts. The inhibitor may have a regulatory function, and F_6 is essential for binding F_1 to the membrane sector, but the roles of the other subunits are obscure.

The ATP synthases of eubacteria, chloroplasts, and mitochondria have related structures and mechanisms. They are membrane-bound enzymes that catalyze ATP production from ADP and inorganic phosphate by using the transmembrane potential gradient for protons, $\Delta\tilde{\mu}_{H^+}$, to drive the reaction (Mitchell, 1961; Nicholls, 1982). In bacterial enzymes and in reconstituted mitochondrial enzymes the process is reversible, and the enzymes can hydrolyze ATP and use the energy released to pump protons. The enzymes from these various sources differ in the complexity of their subunits. To date, the simplest ATP synthase to be described is that from *Escherichia coli* (Fillingame, 1981). It has eight different subunits; five of them, α, β, γ, δ, and ϵ, for a globular domain, F_1-ATPase, which lies outside the membrane, and the three others, a , b, and c, comprise the membrane sector of the enzyme to which F_1 is bound. The enzymes from photosynthetic chloroplasts and bacteria are slightly more complex and appear to have nine subunits (Pick & Racker, 1979; Westhoff

‡The genetic sequence reported for the e subunit of F_1F_O-ATPase has been submitted to GenBank under Accession Number J05330.
*To whom correspondence should be addressed.
§Present address: Academic Medical Centre, University of Amsterdam, 1105 AZ Amsterdam, The Netherlands.
∥R.L. was supported by a long-term EMBO Fellowship and also by a European Science Exchange Fellowship from the Netherlands Organization for Pure Research (N.W.O).
⊥Present address: Laboratoire de Biochimie, LBIO, CENG, BP85X, 38041 Grenoble Cedex, France.

0006-2960/91/0430-5369$02.50/0